PROCEEDINGS OF SCIENCE

ATLAS Planar and 3D Pixel Sensor Performance and Operational Experience at the Large Hadron Collider

Marco Battaglia[a,*] **on behalf of the ATLAS Pixel Detector Collaboration**

[a] *University of California at Santa Cruz*
Santa Cruz Institute for Particle Physics,
1156 High Street, Santa Cruz, CA 95064, USA

E-mail: marco.battaglia@ucsc.edu

This contribution focuses on performance and operating conditions of the ATLAS Pixel detector with special emphasis on radiation damage. It discusses charge collection properties in data and their modelling with radiation damage simulation, 3D sensor performance with comparison to planar sensors as a function of fluence and the efficiency for associating pixel hits to reconstructed charged particle tracks in relation to operation at high rate and mitigation techniques adopted for LHC Run 3.

At particle fluence of O(10^{15}) neutron-equivalent cm^{-2} on the layers closest to the LHC beam pipe, radiation damage has become relevant to most aspects of detector and related physics object performance. ATLAS simulation includes by default a radiation damage pixel digitiser accounting for detailed radiation effects in the Si bulk. The evolution of charge collection efficiency for the innermost barrel pixel layers (IBL and B-Layer) with integrated luminosity and particle fluence has been studied on data and simulation showing good agreement and practicable projections until the end of Run 3. The study of charge collection efficiency for IBL sensors of planar and 3D design confirms the improved response of 3D pixels after irradiation with a gain of $\simeq$ 25-30% in charge collection efficiency at a fluence of 10^{15} n-eq cm^{-2} compared to planar sensors. The efficiency for pixel hits-on-track remains constant with time, thanks to the periodic increase of the operating bias voltage, the optimisation of analog thresholds on innermost layers and the mitigation of de-synchronisation effects at high rate with improved DAQ firmware and software.

The ATLAS Pixel detector performs under conditions that are, for some key parameters (pile-up of 50-60 with tests up to 70 and particle fluence from current 1.0-1.3 $\times$ 10^{15} to 1.5-2.2 $\times$ 10^{15} n-eq cm^{-2} at the end of Run 3) within factors of $\sim$ 3 to 5 compared to the goals for the HL-LHC tracker upgrades. These results already provide useful indications for the optimisation of the operating conditions for the new generation of pixel trackers.

The European Physical Society Conference on High Energy Physics (EPS-HEP2023)
21-25 August 2023
Hamburg, Germany

*Speaker

PoS(EPS-HEP2023)527

1. Introduction

The Pixel detector [1] is the innermost system of the ATLAS Inner Detector (ID) [2]. Its main task is to determine the accuracy of particle track extrapolation to the production vertex. In addition, it provides space points for reconstructing very low momentum particle tracks and measures charged particle dE/dx, important for searches of anomalously ionising new particles. It consists of four barrel layer and three endcap disks installed on either side of the barrel section for a total of 1.9 m^2 of Si in 2024 modules readout through 92 M electronics channels. The innermost layer, the Insertable B Layer (IBL) [3] installed in the shutdown period preceding the start of Run 2, is located at 3.3 cm from the beam axis and is equipped with n+-on-n planar and n+-on-p 3D sensors with 50×250 μm pitch read out by front-end (FE) FEI4 chips in 130 nm CMOS with 4-bit time-over-threshold (ToT) analog information. The other layers and the disks have operated since the start of Run 1 and are equipped with n+-on-n planar sensors with 50×400 μm pitch read out by FEI3 chips in 0.25 μm CMOS with 8-bit ToT analog information.

With 230 fb^{-1} delivered since 2015, IBL received a particle fluence in excess of 10^{15} n-eq cm^{-2} that will increase by a factor of ∼2 by the end of Run 3 in 2025. Radiation damage has become a parameter of relevance in evaluating the performance of the ATLAS pixels and of all the derived physics objects, such as tracking, vertexing and flavour tagging, in event reconstruction and analysis.

2. Charge Collection in Planar Sensors

The pixel charge collection properties are largely determined by radiation damage effects in the Si bulk, in particular on the innermost layers. ATLAS has developed a radiation damage digitiser simulating the charge collection based on realistic E-field maps at different fluences and bias voltages [4, 5]. This digitiser has been adopted in the official MC simulation for Run 3. The fluence values used in the simulation are obtained from the integrated delivered luminosity and a conversion value extracted from the study of the detector leakage current weighted over the longitudinal z coordinate according to the observed distribution of the IBL hits in z of the selected tracks. The main systematic and parametric uncertainties on the collected charge predicted by simulation are due to the electron trapping rate as a function of fluence and to the conversion of integrated LHC delivered luminosity to neutron-equivalent particle fluence on the sensor surface.

Results on the distributions of charge and number of pixels in the clusters on the two innermost layers (IBL and B-Layer) in data and simulation at the start of Run 3 are presented in [6]. Here the charge collection efficiency (CCE) is studied as a function of the integrated delivered LHC luminosity and the fluence. This study provides a validation of the simulation predictions over a wide range of luminosity and fluence values and an important estimate of the response during the residual operating life of the ATLAS pixels until the end of Run 3. The CCE is defined as the fitted most probable value (MPV) of the cluster charge for hits associated to reconstructed tracks and corrected by the particle path in Si normalised to the same quantity measured at the beginning of Run 2 in 2015 for IBL and of Run 1 in 2010 for B-Layer. Results are summarised in Figure 1. The simulation shows good agreement with data for both IBL and B-Layer, within the estimated uncertainties, over almost two orders of magnitudes of particle fluences. By regularly increasing

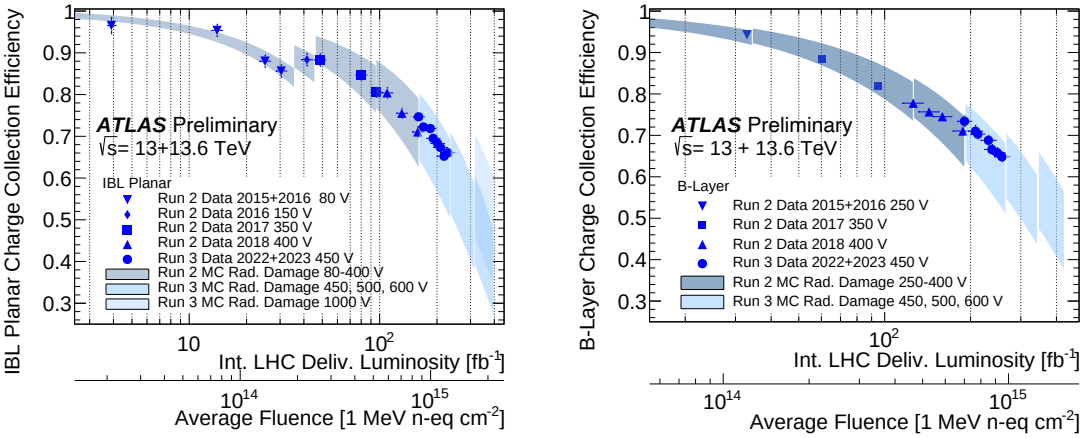

Figure 1: Charge collection efficiency (CCE) and radiation damage for planar sensors. Estimated CCE as a function of the integrated delivered luminosity and particle fluence for IBL (left panel) and B-layer (right panel) planar sensors since the beginning of Run 2. The points represent the data and the bands the simulation predictions with their uncertainty. Sudden increases in charge collection efficiency at the beginning of each year are due to changes in the operational parameters (bias voltage and thresholds). Predictions for the CCE evolution in 2024 and 2025 are also given (from ref.[7]).

the bias voltage, the charge collection efficiency on innermost layers can be kept within ~50% of the original value until end of Run 3, assuming a total integrated luminosity for Run 2+3 of ≃400 fb^{-1}.

3. Performance of 3D Sensors

Pixels of 3D design represent one of the most innovative developments from the R&D effort towards pixel sensors delivering the performance required by the LHC physics program while coping with the radiation levels. The 3D design adopts a sensor geometry with column electrodes penetrating the Si substrate instead of being implanted on the wafer surface, as in the planar design [8]. The first 3D pixel sensors installed in an LHC experiment are those at the outer ends of the staves of the IBL [9], covering the longitudinal region, along the beam axis, of 245< $|z|$ <335 mm, corresponding to particles in the pseudo-rapidity range of 1.90< $|\eta|$ <2.55, accounting for the beam-spot size.

Pixels of 3D design are intrinsically more tolerant to bulk damage, due to the reduced charge drift path from the point of energy deposition to the collecting electrode and consequently reduced collection time, ~0.5 ns for the IBL 3D vs. ~0.9 ns for the IBL planar pixels for e^- after 10^{15} n-eq cm^{-2}, without reducing the thickness of the traversed active Si material and, thus, the signal charge. These qualities made 3D pixels a technology of choice for the tracker upgrades pursued in preparation for the HL-LHC program. Results from their first operation at LHC in Run 2 and 3 provide a number of useful inputs for future optimisation and developments.

Radiation damage effects in the Si bulk of 3D pixel sensors are simulated in the ATLAS pixel radiation damage digitiser, as for the planar sensors discussed in the previous section. The electric field profiles for 3D pixels are also simulated with TCAD but, in contrast to planar sensors, the field in 3D sensors is nearly independent of the depth and depends strongly on the position on the sensor surface. Compared to planar sensors, electrons and holes follow non-trivial trajectories from

the ionisation point to their collection on the n+ implant, due to the more complex shape of this electric field. However, a simplification is afforded, since the electric field is nearly parallel to the magnetic field and the Lorentz angle is negligibly small. The computation of the Ramo potential for 3D sensors is also more complex than that for planar sensors because the calculation requires a relatively large simulation area. Simulation predictions from the radiation damage digitiser have been compared to data collected towards the end of Run 2, after 156.5 fb^{-1} of integrated luminosity, corresponding to an average fluence of approximately 5.1 $\times 10^{14}$ n-eq cm^{-2}. The distributions of the cluster charge for data and simulation are shown in Figure 2. The change in the collected charge with the applied bias voltage has been studied in periodic voltage scans during Run 2 and 3. These show a moderate increase of the depletion voltage since the beginning of 2016, corresponding to an integrated luminosity of 5 fb^{-1}, to that of 2023, at an integrated luminosity of 185 fb^{-1}, together with the slope of charge increase above depletion, due to the increase of the charge trapping effect with charge carrier velocity (see Figure 2).

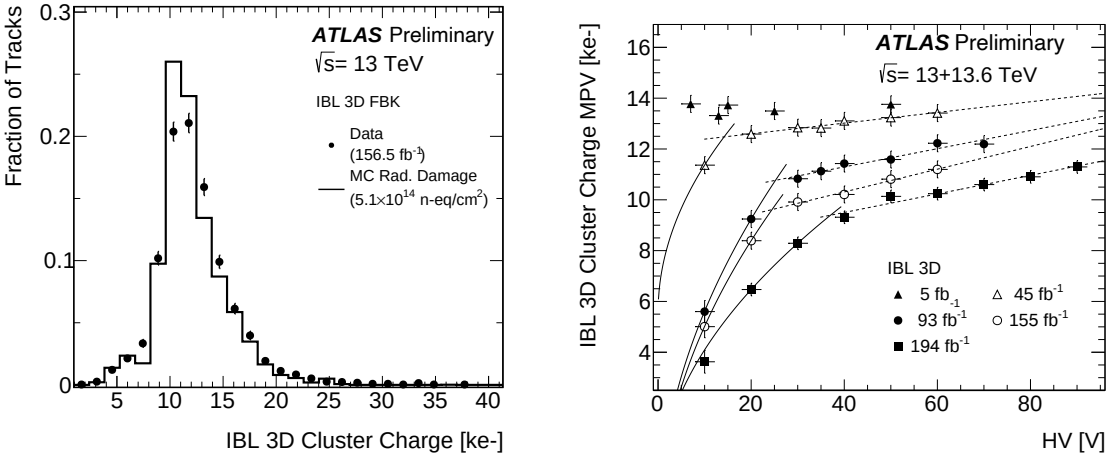

Figure 2: Charge collection in irradiated IBL 3D sensors. Left: Pixel cluster charge, corrected by the particle path in Si, for clusters associated to reconstructed particle tracks. Points with error bars represent data in 13 TeV collisions collected in 2018 after 156.5 fb^{-1} of integrated luminosity compared to the simulation predictions using the model of ref. [10]. Right: Cluster charge MPV as a function of the detector bias voltage (HV). Points represent data recorded during bias voltage scans from early 2016 to end of 2022, after integrated delivered luminosities from 5 to 185 fb^{-1}, corresponding to average particle fluences from 0.2 to 6 $\times 10^{14}$ n-eq cm^{-2}. The lines represent $\sqrt{V}$ (continuous) and linear (dashed) fitted functions, modelling the increase in charge collection efficiency in the regimes below and above the depletion point (from ref. [11]).

The reduced sensitivity of 3D pixels to radiation damage effects can be tested by studying the change of CCE with integrated luminosity and fluence. The CCE values for data and radiation damage simulation have been computed for 3D pixels, as discussed above for planar sensors and results are summarised in Figure 3. There is good agreement between data and radiation damage simulation. The IBL 3D pixels show an improved response in terms of charge collection efficiency compared to IBL planar sensors, whose performance is shown in the left panel of Figure 1, at the same fluence. Taking a fluence benchmark at 10^{15} n-eq cm^{-2}, not yet reached by the IBL 3D pixels, we observe a 25-30% gain for 3D compared to planar sensors.

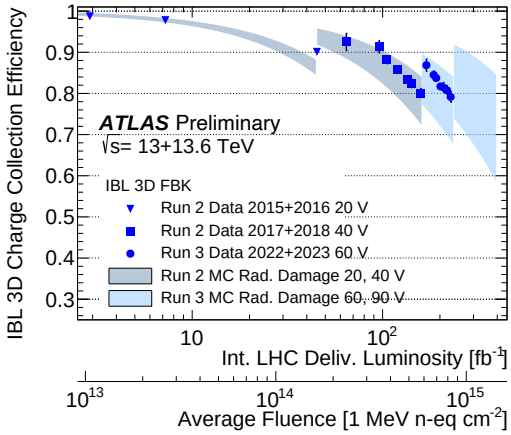

Figure 3: Charge collection efficiency and radiation damage for 3D sensors. Same as Figure 1, for IBL 3D sensors (from ref. [7]).

4. Hits-On-Track Efficiency and Operational Performance at High Rate

The hit-on-track efficiency drives the performance of tracking and of the derived physics objects. The periodic optimisation of the operating bias voltage and analog thresholds has ensured a uniform response of the Pixel detector in terms of hit-on-track efficiency so far. The pixel efficiency has been measured to be constant within ≤2% on all layers throughout Run 2 [12]. The hit-on-track efficiency must also be preserved in pixel operations under challenging LHC conditions, in particular pile-up (PU) during Run 3, inducing effects related to module de-synchronisation and bandwidth limitations. De-synchronisation effects reducing the hit-on-track rate, in particular on the B-Layer,

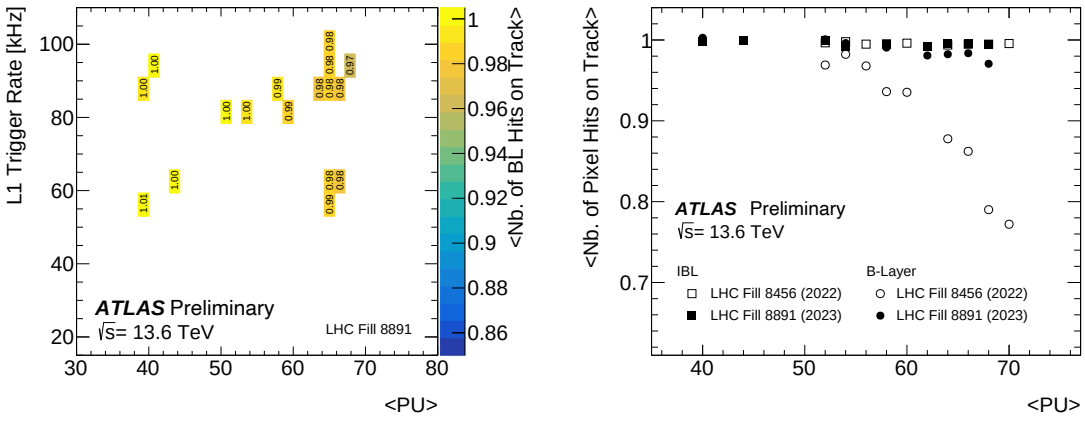

Figure 4: Pixel hit-on-track efficiency and data taking conditions. (Left) Average number of B-Layer hits associated to reconstructed particle tracks as a function of the L1 trigger rate and average PU in 2023. (Right) Average number of IBL (squares) and B-Layer (circles) hits associated to reconstructed particle tracks as a function of the average PU. Data were collected during special fills in 2022 (LHC fill 8456, shown by the open markers) and 2023 (LHC fill 8891, shown by the filled markers), where the values of PU and trigger rate were scanned to study the detector response. The improved response of the B-Layer is due to the upgrades in the DAQ firmware and software, as well as the analog threshold optimisation (from ref. [13]).

have been observed at high values of PU and/or Level-1 (L1) trigger rate, more noticeably since

the start of Run 3. A uniform response from IBL has ensured a constant efficiency and quality for reconstructed tracks.

In 2023, an effective de-synchronisation mitigation has been achieved by optimising the B-layer analog thresholds and introducing new features in the DAQ firmware and software. These temporarily veto triggers for modules overloaded with hits in buffers and reconfigure all FE global and pixel registers every 5 s, without adding dead-time, to recover from single event upset (SEU) effects. Commissioned in steps during the 2023 data taking, these upgrades minimise the de-synchronisation effects and improve the hit-on-track efficiency (see Figure 4), thus re-establishing a constant efficiency response vs. pile-up.

References

[1] G. Aad *et al.*, *ATLAS pixel detector electronics and sensors*, *JINST* **3** (2008), P07007.

[2] ATLAS Collaboration, *The ATLAS Experiment at the CERN Large Hadron Collider*, *JINST* **3** (2008), S08003.

[3] ATLAS IBL Collaboration, *Production and Integration of the ATLAS Insertable B-Layer*, *JINST* **13** (2018), T05008.

[4] ATLAS Collaboration, *Modelling radiation damage to pixel sensors in the ATLAS detector*, *JINST* **14** (2019), P06012.

[5] M. Bomben, these proceedings.

[6] ATLAS Collaboration, *Performance of ATLAS Pixel Detector and Track Reconstruction at the start of Run 3 in LHC Collisions at* $\sqrt{s}$*=900 GeV*, ATL-PHYS-PUB-2022-033.

[7] ATLAS Collaboration, *Charge Collection Efficiency for the ATLAS Planar and 3D Pixel Sensors in Collision Data and Radiation Damage Simulation*, ATLAS-PIX-2023-001.

[8] S. Parker, C.J. Kenney and J. Segal, *3D - A proposed new architecture for solid-state radiation detectors* *Nucl. Instrum. Meth.* **A395** (1997), 328.

[9] C. Da Via *et al.*, *3D silicon sensors: Design, large area production and quality assurance for the ATLAS IBL pixel detector upgrade*, *Nucl. Instrum. Meth.* **A694** (2012), 321.

[10] A. Folkestad *et al.*, *Development of a silicon bulk radiation damage model for Sentaurus TCAD*, *Nucl. Instr. and Meth.*, **874** (2017), 94.

[11] ATLAS Collaboration, *Validation of Radiation Damage Simulation for Charge Collection in the ATLAS IBL 3D Pixel Sensors with 13 TeV Collision Data*, ATLAS-PIX-2023-002.

[12] ATLAS Collaboration, *Pixel Hit-on-track Efficiency, Average Occupancy and Fraction of Disabled Modules for Run 2*, ATLAS-PIX-2020-003.

[13] ATLAS Collaboration, *Pixel Hit-on-Track Efficiency and Running Conditions in 2023*, ATLAS-PIX-2023-003.